Title

Ultrastructure and cardiac impulse propagation: scaling up from microscopic to macroscopic conduction.

Permalink

Authors

Qu, Zhilin

Hanna, Peter

Ajijola, Olujimi

et al.

Publication Date

DOI

TOPICAL REVIEW

Ultrastructure and cardiac impulse propagation: scaling up from microscopic to macroscopic conduction

Zhilin Qu ⃝, Peter Hanna ⃝, Olujimi A. Ajijola ⃝, Alan Garfinkel ⃝ and Kalyanam Shivkumar ⃝

UCLA Cardiac Arrhythmia Center and Department of Medicine, David Geffen School of Medicine, University of California, Los Angeles, California, USA

Handling Editor: Harold Schultz & David Paterson

The peer review history is available in the Supporting Information section of this article (https://doi.org/10.1113/JP287632#support-information-section).
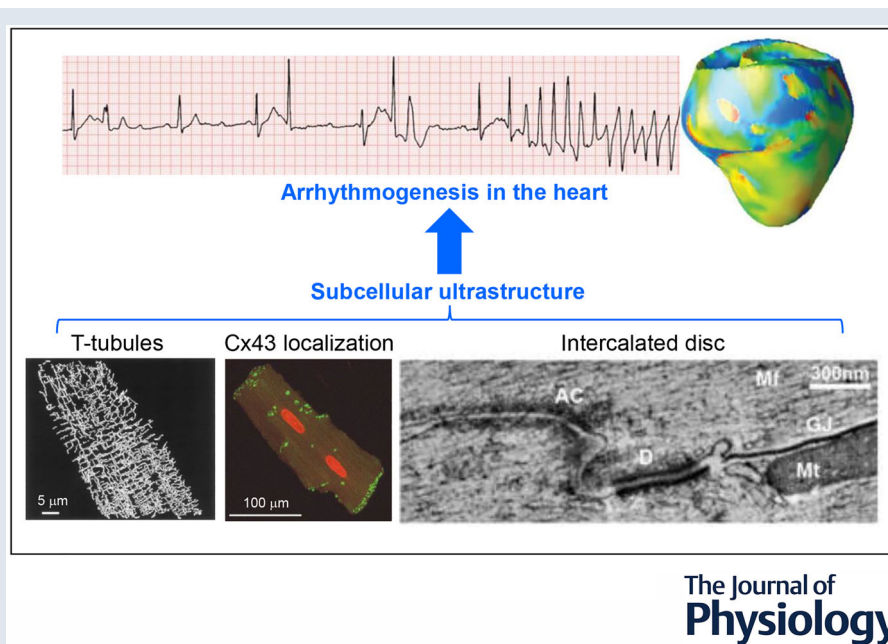
Abstract figure legend Scaling up ultrastructural heterogeneities and subcellular conduction to arrhythmogenesis in the heart. Lower panels: T-tubular network in a ventricular myocyte (left); Cx43 distribution (green) in a ventricular myocyte (middle); and in an intercalated disc linking two myocytes. AC, area composita; D, desmosome; GJ, gap junction; Mf, myofibrils; and Mt, mitochondria. Upper panels: ECG showing initiation of arrhythmias (left) and colour map of voltage of the epicardial surface during an arrhythmia from a computer simulation (right).

Zhilin Qu earned his PhD in physics from Beijing Normal University and completed his post-doctoral training at the University of California, Los Angeles (UCLA). He is currently a Professor of Medicine and Computational Medicine at UCLA. His research focuses on the mechanisms of cardiac arrhythmias, utilizing computer modelling and non-linear dynamical theories, in close collaboration with experimentalists and clinicians. **Kalyanam Shivkumar** received his medical degree from the University of Madras, India, and his PhD from UCLA. He completed his cardiology fellowship at UCLA and is currently a Professor of Medicine and Radiology, as well as the director of the UCLA Cardiac Arrhythmia Center. His specialization is in interventional cardiac electrophysiology and innovative techniques for the non-pharmacological management of cardiac arrhythmias. His research focuses on the mechanisms of cardiac arrhythmias in humans, particularly the role of the autonomic nervous system.
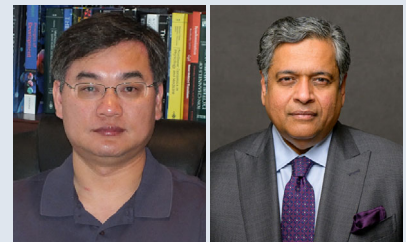
Abstract The standard conception of cardiac conduction is based on the cable theory of nerve conduction, which treats cardiac tissue as a continuous syncytium described by the Hodgkin–Huxley equations. However, cardiac tissue is composed of discretized cells with microscopic and macroscopic heterogeneities and discontinuities, such as subcellular localizations of sodium channels and connexins. In addition to this, there are heterogeneities in the distribution of sympathetic and parasympathetic nerves, which powerfully regulate impulse propagation. In the continuous models, the ultrastructural details, i.e. the microscopic heterogeneities and discontinuities, are ignored by 'coarse graining' or 'smoothing'. However, these ultrastructural components may play crucial roles in cardiac conduction and arrhythmogenesis, particularly in disease states. We discuss the current progress of modelling the effects of ultrastructural components on electrical conduction, the issues and challenges faced by the cardiac modelling community, and how to scale up conduction properties at the subcellular (microscopic) scale to the tissue and whole-heart (macroscopic) scale in future modelling and experimental studies, i.e. how to link the ultrastructure at different scales to impulse conduction and arrhythmogenesis in the heart.

Introduction

Cardiac contraction is originated by electrical impulses generated from the sinoatrial node, which conduct to the atria, atrioventricular node, the His-Purkinje system and, finally, the ventricles. Current theories of cardiac conduction are based mainly on the continuous cable model of nerve conduction developed by Hodgkin and Huxley (1952). The Hodgkin–Huxley equations were modified or extended to describe ionic currents and action potential dynamics in single cardiac cells, impulse conduction in a one-dimensional (1D) cable, two-dimensional (2D) and three-dimensional (3D) tissue, as well as anatomically based whole-heart models (Qu et al., 2014). Mechanistic insights and theories derived from the continuous models have been used to explain experimental and clinical observations, which have greatly improved our understanding of cardiac conduction in general.

However, cardiac tissue is composed of discretized cells that are coupled electrically, and the continuous models may not describe the conduction dynamics properly, particularly under disease conditions. In the continuous cable theory, cardiac tissue is treated as a syncytium, ignoring the subcellular localizations of ion channels and ultrastructures at the cellular and tissue scales. Computational models incorporating detailed discretized structural information have been developed to investigate their effects on cardiac conduction. In this article, we discuss current progress and the issues or challenges faced by the cardiac modelling community to scale up the conduction properties at the sub- cellular (microscopic) scale to the tissue and whole-heart (macroscopic) scale, i.e. how to link the emerging data on ultrastructure at different scales to impulse conduction and arrhythmogenesis in the heart.

Ultrastructure in the heart

Cardiac myocytes are elongated cells with irregularly varying shapes and sizes (Fig. 1*A*). Myocytes in cardiac muscle form an irregular myocyte network in which a myocyte is connected to a number of others. For example, in normal canine ventricular tissue, one myocyte is connected on average to 11 other myocytes (Hoyt et al., 1989; Peters & Wit, 1998). Myocytes are electrically and mechanically coupled via connections at the intercalated discs (IDs) (Leo-Macías et al., 2015; Nielsen et al., 2023). The IDs are located at the cell ends, which contain three types of junctions: adherens, desmosomes and gap junctions (Fig. 1*B*). Adherens and desmosomes provide strong myocyte adhesion to resist shearing force during contraction and mechanical coupling for mechanical energy transmission. Gap junctions facilitate electrical coupling for electrical impulse conduction. Gap junctions are hemichannels composed of connexin (Cx) proteins (Desplantez et al., 2007). The known connexins expressed in the heart are Cx43, Cx40 and Cx45. Ventricular tissue mainly expresses Cx43; atrial tissue expresses both Cx43 and Cx40. Cx45 can be detected in both the ventricular and atrial myocardium at very low levels. In normal adult hearts, gap junctions mainly localize in the IDs at the cell ends with a small portion laterally (Fig. 1*C*). Under disease

conditions, such as in heart failure and ischaemia, or in young and aged hearts, lateral Cx43 is more abundant, a phenomenon referred to as Cx43 lateralization (Hesketh et al., 2010; Martins-Marques et al., 2020; Saffitz et al., 2007; Severs et al., 2008; Vreeker et al., 2014). Besides its role in forming gap junctions, Cx43 also exhibits non-gap junction functions (Leo-Macias, Agullo-Pascual, Delmar, 2016; Rhett et al., 2011), such as regulating ionic currents. For example, the sodium (Na^+) current I_{Na} becomes smaller in Cx43-deficient myocytes (Jansen et al., 2012).

Besides Cx43 subcellular localization, ion channels are also distributed heterogeneously within a myocyte. For example, the cardiac isoform of the Na^+ channel ($Na_v1.5$) is more densely expressed in the IDs than in the lateral sarcolemmal (SL) membrane (Lin et al., 2011; Vreeker et al., 2014). This is consistent with the observation that $Na_v1.5$ colocalizes with Cx43 (Fig. 1*D*) and adherens (Leo-Macias, Agullo-Pascual, Sanchez-Alonso, et al., 2016; Maier et al., 2004; Raisch et al., 2018). Furthermore,

the kinetics of Na^+ channels in the IDs are different from those in the lateral SL membrane, the steady-state activation curve shifts to more negative voltages, and the steady-state inactivation curve shifts to more positive voltage (Lin et al., 2011; Weinberg, 2023). In addition to the heterogeneous distribution within the SL, $Na_v1.5$ and other ion channels also distribute differently between the SL and T-tubular membranes. T-tubules are subcellular structures in atrial and ventricular myocytes, invaginations of the sarcolemma membrane that form a T-tubular network inside the cell (Brandenburg et al., 2016; Soeller & Cannell, 1999; Song et al., 2006, 2018). In normal ventricular myocytes, there is a well-organized T-tubular network (Fig. 2*A*), whose membrane accounts for 21–64% of the total membrane of the myocyte, based on different studies (Hong & Shaw, 2017). Under disease conditions, such as heart failure (Guo et al., 2013; Lyon et al., 2009; Sachse et al., 2012; Song et al., 2006), the T-tubular system is disrupted, resulting in a less
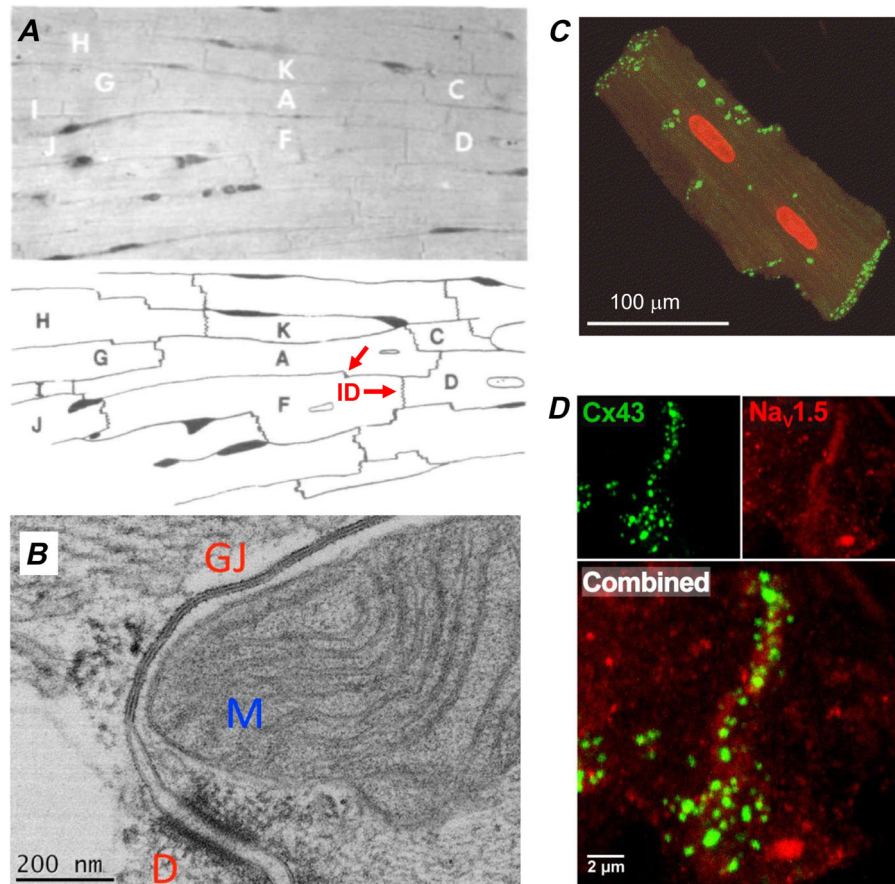
Figure 1. Subcellular and cellular ultrastructure
A, light micrograph of cardiac muscle fibres from a canine myocardium (upper) and a drawing of the myocytes showing myocyte connections at intercalated discs (IDs, examples labelled by arrows). Adapted from Hoyt et al. (1989). *B*, transmission electron microscopy image of the adult murine heart showing gap junctions (labelled as 'GJ'), desmosomes (labelled as 'D') and mitochondria (labelled as 'M'). Adapted from Delmar and Liang (2012). *C*, Cx43 clusters in intercalated discs in an isolated ventricular myocyte. Adapted from Severs et al. (2004). *D*, colocalization of Cx43 (green) and $Na_v1.5$ (red) in IDs. Adapted from Raisch et al. (2018).

dense and more irregular T-tubular network (Fig. 2*B*). Remodelling of the T-tubular system alters not only excitation–contraction (E–C) coupling dynamics (Nivala et al., 2015) but also the excitation itself (Fig. 2*C*) (Sacconi et al., 2012). In atrial myocytes, the T-tubular networks are usually much less dense and very heterogeneous between regions in the same heart (Arora et al., 2017; Frisk et al., 2014; Glukhov et al., 2015; Kirk et al., 2003) and between species (Richards et al., 2011). Purkinje fibre cells are largely free of T-tubules (Boyden et al., 1989; di Maio et al., 2007; Legato, 1973). T-tubules are also largely absent in myocytes in early development, in cultured myocytes and in stem-cell derived cardiac myocytes (Brette & Orchard, 2003; Chen et al., 1995; Lieu et al., 2009; Lipp et al., 1996; Liu et al., 2009). Brette & Orchard (2006, 2007) performed quantitative analyses of ion channel distribution between the SL and the T-tubular membrane in rat ventricular myocytes. They estimated that the T-tubular membrane accounts for only 30% of the total membrane of a rat ventricular myocyte, but contains 80% of the calcium (Ca^{2+}) and 63% of the Na^+–Ca^{2+} exchange currents. $Na_v1.5$ is slightly denser in the SL than in the T-tubular membrane. Besides the cardiac isoform

($Na_v1.5$), ventricular myocytes also contain three neural isoforms of the Na^+ channel ($Na_v1.1$, $Na_v1.3$ and $Na_v1.6$) (Brette & Orchard, 2006; Kaufmann et al., 2013; Maier et al., 2002, 2004), which are predominantly found in the T-tubules. The neural isoforms account for roughly a quarter of the Na^+ channels in the T-tubules and 10% of the Na^+ channels of the whole cell. The subcellular $Na_v1.5$ channel distribution also changes under disease conditions (Petitprez et al., 2011; Rivaud et al., 2017).

Cardiac myocytes are coupled mechanically through the IDs that are mainly located at the cell ends, and thus they align in certain ways (Fig. 1*A*) to form myocyte fibres that optimize contractile function. The fibre directions rotate in the heart transmurally and from apex to base (Nielsen et al., 1991; Scollan et al., 2000; Streeter et al., 1969). In many tissue or whole-heart simulations incorporating fibre structures (Liu et al., 2019; Trayanova, 2011; Xie et al., 2004), continuous tissue models are used. However, the myocyte fibres form sheets and bundles with discontinuous or laminar structures (Fig. 2*A*), which cause discontinuous conduction in the heart and can also impact defibrillation (Hooks et al., 2002, 2007).
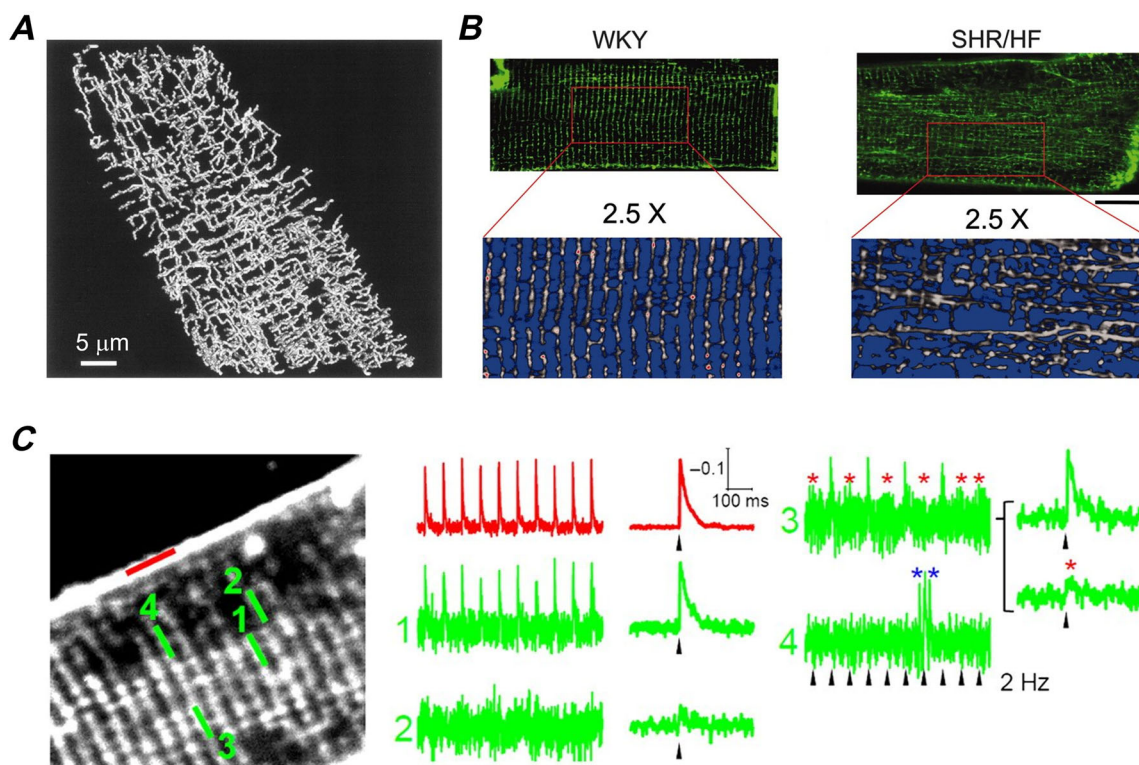
Figure 2. T-tubular structures and intracellular action potential conduction
A, a 3D view of T-tubular network in a rat ventricular myocyte, adapted from Soeller and Cannell (1999). *B*, T-tubule remodelling in heart failure, adapted from Song et al. (2006). *C*, action potential conduction in a failing myocyte. Left: representative transmembrane image of a heart failure myocyte. Right: normalized fluorescence traces from the scanned line indicated in the left panel: SS and TT1 show regular action potentials, TT2 and TT3 display non-regenerative electrical responses, and TT4 highlights local arrhythmic events (blue asterisks). Adapted from Sacconi et al. (2012).

The conduction of electrical impulses from the atrioventricular node to the ventricles is via the His-Purkinje fibre network (Fig. 2*B*), a complex structure (Atkinson et al., 2011; Liu & Cherry, 2015) that facilitates synchronous excitation and contraction of the ventricles. A key issue is the coupling of Purkinje fibre cells with ventricular myocytes: they need to be coupled in a way that maintains the fast conduction in the Purkinje fibre network but overcomes the source–sink effect to activate the ventricles. While ventricular myocytes and the Purkinje network constitute the necessary components for the working ventricles, there are other types of cells that play non-trivial roles in cardiac E–C coupling and arrhythmogenesis, such as neural cells (Fukuda et al., 2015; Kawano et al., 2003). The neural cells or nerve fibres exhibit a dense distribution, intermingled with myocytes in the heart (Fig. 2*C*) (Zhu et al., 2022). Moreover, nerve fibres may send processes through the myocyte, i.e. a nerve fibre may penetrate the cell membrane to locate inside the cell (Fig. 2*D*). Under disease conditions, neural remodelling results in more heterogeneous nerve fibre distributions (Ajijola et al., 2013; Cao et al., 2000; Chang et al., 2001; Dajani et al., 2023). Fibroblasts are another type of cell that can exhibit non-trivial electrophysiological effects in the heart (Camelliti et al., 2005; Wang et al., 2023; Xie et al., 2009), which can become more prominent in cardiac diseases, such as ischaemia.

Subcellular action potential conduction

In the continuous cable theory models, the subcellular and cellular ultrastructural details are ignored by 'coarse graining' or 'smoothing'. In computer simulations, the continuous models are discretized into coupled 'computational cells', either uniformly or in the form of brick walls (Hubbard et al., 2007; Xie et al., 2009).
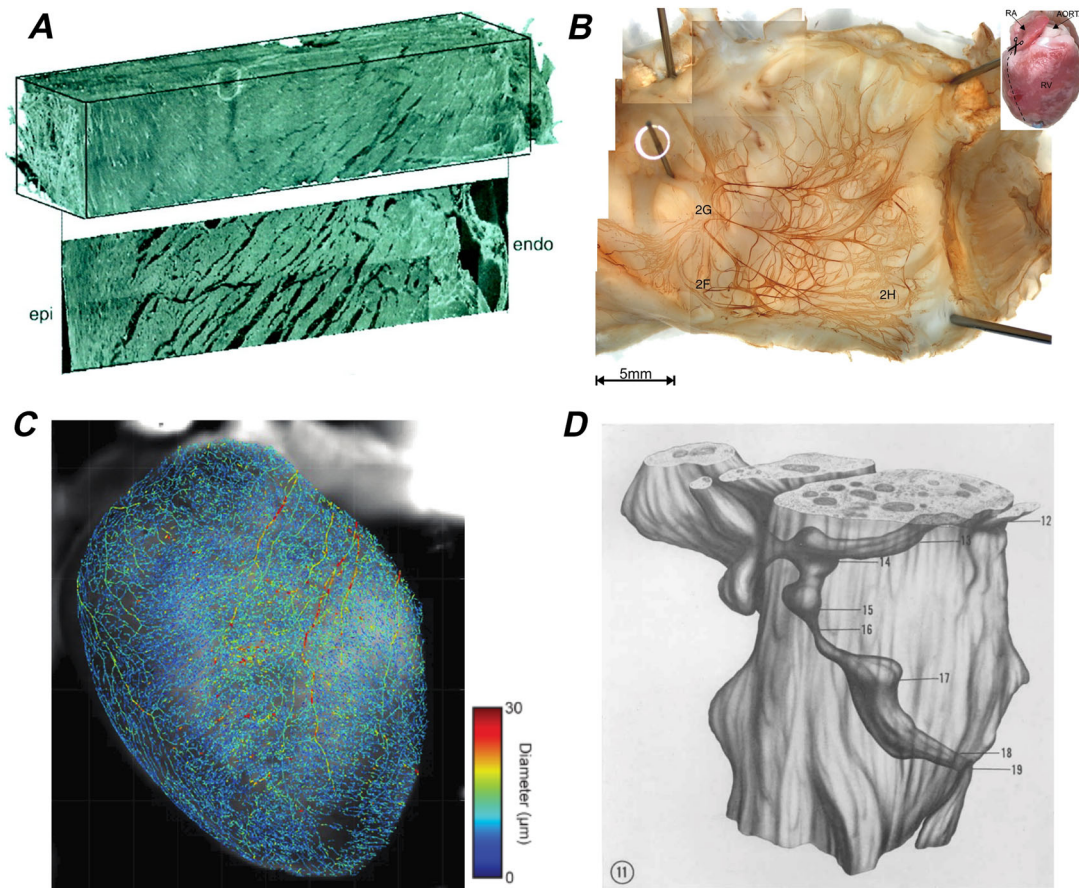
Figure 3. Tissue- and organ-scale ultrastructure
A, Upper: reconstructed volume of rat left ventricular free-wall myocardium. Lower: transmural slice from the reconstructed volume showing a complex network of cleavage planes that course between layers of myocytes. Each layer is of an order of 80 μm in thickness. Adapted from Hooks et al. (2002). *B*, His-Purkinje network (dark brown) in a rabbit heart. Adapted from Atkinson et al. (2011). *C*, high-magnitude image of nerve fibre distribution in the heart. Colour is the diameter of the nerve as indicated by the colour bar. Adapted from Zhu et al. (2022). *D*, constructed electron micrograph showing a vesiculated nerve (dark colour) process within a sarcolemma-lined tunnel inside a nodal cell. Adapted from Thaemert (1970).

The membrane potential in a 'computational cell' is uniform without subcellular heterogeneities. However, the structural heterogeneities at the subcellular scale can still be important for conduction at the tissue scale. For example, due to the heterogeneities in the T-tubular network, depolarizations of the T-tubular membrane and SL membrane may not be synchronous, as shown in optical mapping experiments (Fig. 3C). Therefore, the T-tubular network affects not only E–C coupling but also electrical conduction at the subcellular scale, which eventually affects conduction at the tissue and organ scales. Besides T-tubules, there are other intracellular structural heterogeneities that may impact E–C coupling and action potential conduction. However, even without the subcellular heterogeneities, heterogeneous localization of Cx43 can result in complex subcellular action potential conduction (Fig. 4), as demonstrated in computer models by Spach & Heidlage (1995) and Spach et al. (2000).

The perinexus, ephaptic coupling and beyond

The ID is the specialized structure coupling cardiac myocytes mechanically and electrically, and is a highly complex structure (Hoyt et al., 1989; Leo-Macías et al., 2015; Leo-Macias, Agullo-Pascual, Sanchez-Alonso, et al.,

2016; Pinali et al., 2015; Vanslembrouck et al., 2020; Zhang et al., 1996). Namely, the ID exhibits a tortuous and plicate structure (Fig. 5A) which contains gap junctions, adherens and desmosomes (Fig. 5B). In the gap junction regions (Figs 1B and 5B), the cell membranes are closely positioned (∼2 nm) to allow formation of the gap junctions. Close to the gap junction region, the adjacent cell membranes have larger separations, ranging from 2 to 100 nm, where adherens and desmosomes are located. The region in close proximity to the gap junction region is called the perinexus (Fig. 5C), a term coined by Rhett and colleagues (Gourdie, 2019; Rhett and Gourdie, 2012; Rhett et al., 2013). High-resolution imaging showed that $Na_v1.5$ in this region is colocalizing with other proteins, such as Cx43 and adhesion proteins (Leo-Macias, Agullo-Pascual, Sanchez-Alonso, et al., 2016; Rhett et al., 2012; Veeraraghavan et al., 2015).

While gap junction coupling for myocyte-to-myocyte conduction has been the mainstream theory for cardiac conduction, an alternative theory, called ephaptic coupling, has been in existence for decades, first proposed by Sperelakis and Mann in 1977 (Sperelakis, 2002; Sperelakis & Mann, 1977). In this theory, a direct current flow from one myocyte to another, as in the case of gap junction coupling, is not required, but rather, conduction occurs via the change of the electrical field between the
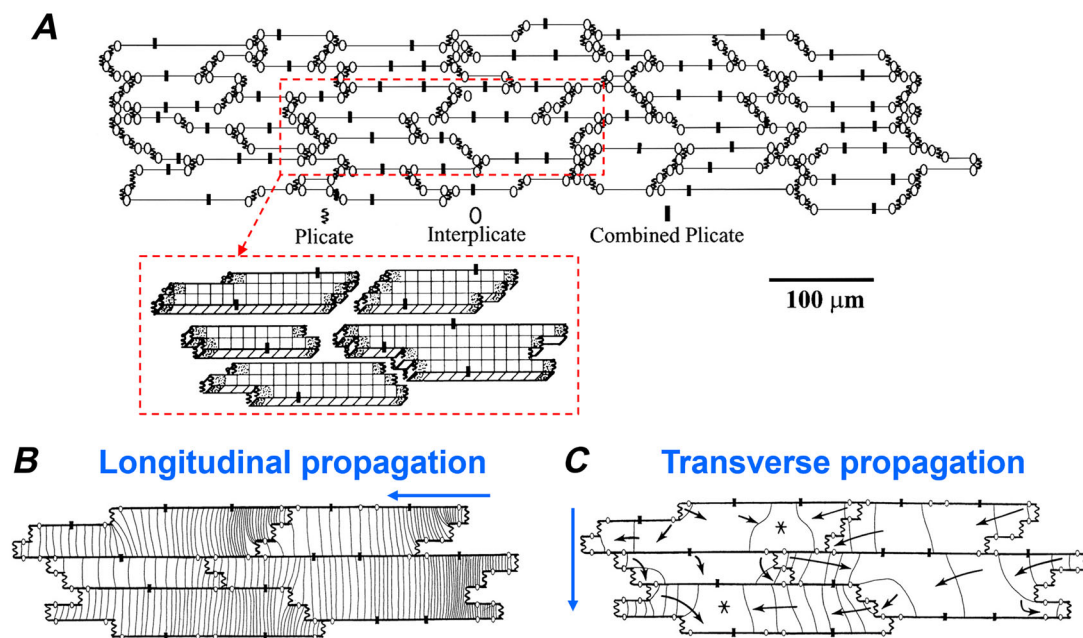
Figure 4. Discontinuous conduction
A, a 2D tissue model consisting of 33 myocytes of different cell sizes and geometries as well as the distribution of gap junctions. The inset below shows computational grids (resolution: $10 \times 10 \times 11.3 \ \mu m^3$) of five cells from the 33-cell tissue. For details of the model see Spach & Heidlage (1995) and Spach et al. (2000). *B*, isochrones within each of the five myocytes during propagation (blue arrow) along the longitudinal axis of the cells. The isochrones are separated by 4 μs. Propagation directions inside the cells are all from right to left. *C*, same as *B* but during propagation (blue arrow) along the transverse axis of the cells. The isochrones are separated by 3 μs. Propagation directions inside the cells are indicated by arrows.

cells during depolarization. That is, the depolarization of one myocyte alters the electrical field or potential in the cleft, which then changes the transmembrane potential of the adjacent myocyte, causing it to depolarize (Fig. 4A). Specifically, opening of the Na$^+$ channel during depolarization of one myocyte (Cell 1) causes Na$^+$ ions to enter the myocyte from the cleft space, lowering the potential of the cleft space (from $\phi_c = 0$ to $\phi_c < 0$). A lower potential of the cleft space then causes an increase in transmembrane potential ($V_{m2} = \phi_{i2} - \phi_c$) of the other cell (Cell 2). Once V_{m2} reaches the Na$^+$ channel activation threshold, the Na$^+$ channels in Cell 2 open to depolarize the cell, resulting in conduction from Cell 1 to Cell 2. According to computer modelling studies (Kucera et al., 2002; Lin & Keener, 2010), for ephaptic coupling to occur, it requires sufficiently many Na$^+$ channels in the cleft membrane and a proper volume of the cleft space (or distance between the two cells). The perinexus is the physical entity that can satisfy the volume requirement and the presence of enough Na$^+$ channels.

Ephaptic coupling has been demonstrated in many modelling studies (Greer-Short et al., 2017; Hichri et al., 2018; Ivanovic & Kucera, 2021, 2002, 2022; Lin & Keener, 2010; Ly & Weinberg, 2022; Moise et al., 2021; Mori et al., 2008; Wang et al., 2023; Wei & Tolkacheva, 2020; Weinberg, 2023). Although a direct experimental demonstration is still not available, indirect experimental evidence has been shown under different conditions, mainly by Poelzing and colleagues (Adams et al., 2023; Blair et al., 2024; George et al., 2016; Raisch et al., 2018; Veeraraghavan et al., 2015, 2016). In these experimental studies, the main experimental approach is to alter the volume of the perinexus using chemical agents to observe their effects on conduction velocities.
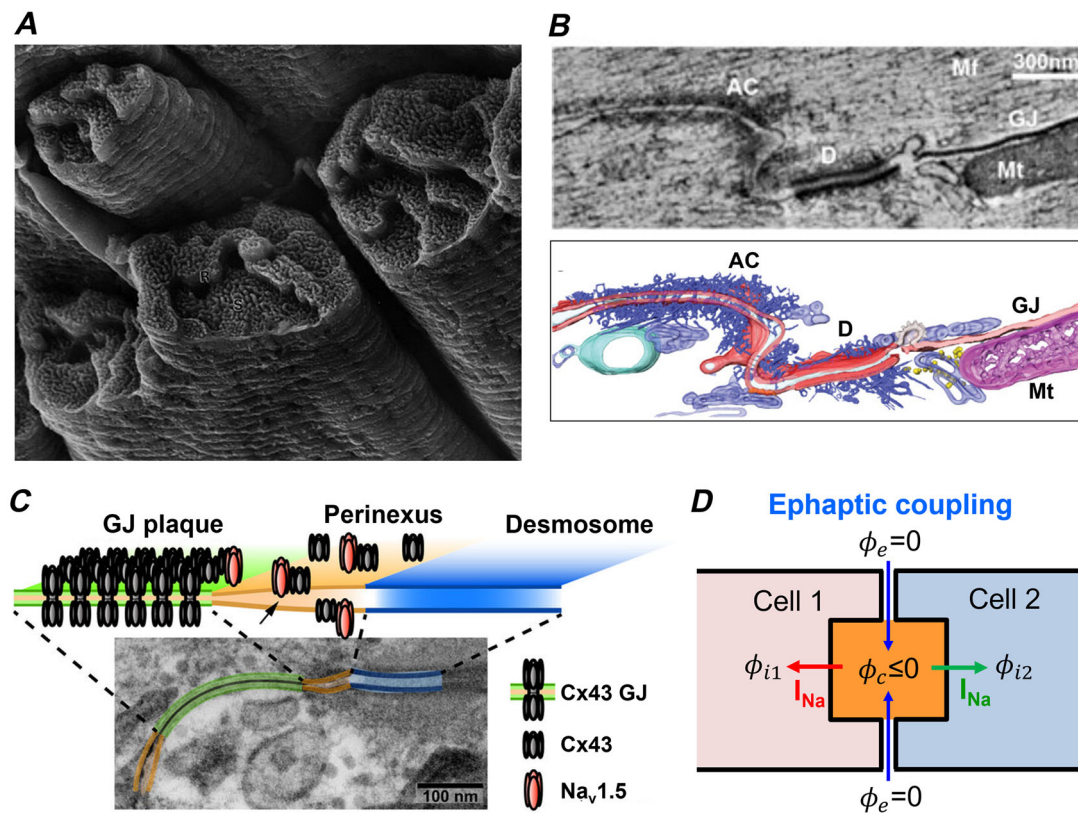
Figure 5. Perinexus and ephaptic coupling
A, scanning electron microscopy image of IDs in monkey ventricular myocytes. Adapted from Zhang et al. (1996). *B*, tomographic electron microscopy section and 3D rendered representation of a portion of the intercalated disc of mouse ventricular tissue. Top: virtual section of tomogram showing different typical ID structures: AC, area composita; D, desmosome; GJ, gap junction; Mf, myofibrils; and Mt, mitochondria. Bottom: a 3D rendered model of the ID. Adapted from Leo-Macias, Agullo-Pascual, Delmar (2016). *C*, schematic diagram illustrating the structural organization of channels within the perinexus. The transmission electron micrograph with the gap junction is highlighted in green, the perinexus in orange and the desmosome in blue. Adapted from Rhett et al. (2013). *D*, schematic diagram illustrating ephaptic coupling. Depolarization of Cell 1 causes Na$^+$ ions to enter Cell 1 from the cleft or perinexus (orange), which lowers the potential in the cleft (ϕ_c). The lowering of ϕ_c results in an increase in transmembrane potential ($V_{m2} = \phi_{i2} - \phi_c$) of Cell 2. Once V_{m2} is higher than the Na$^+$ channel activation threshold, the Na$^+$ channels activate, depolarizing Cell 2.

Besides its roles in ephaptic coupling, the perinexus may also play important roles in repolarization under gap junction coupling. For example, the depletion of Na^+ in the cleft affects the driving force of I_{Na}, which can affect the late component of I_{Na} and thus the late I_{Na}-related repolarization properties (Greer-Short et al., 2017; Nowak et al., 2020, 2021; Wu et al., 2021).

Scaling up microscopic conduction to macroscopic conduction: problems and challenges

Numerical methods using either finite differences or finite element methods are used in computer simulations of continuous tissue models. In the finite difference methods, cells are discretized into coupled 'computational cells', either uniformly or in the form of rectangular brick walls (Hubbard et al., 2007; Xie et al., 2004, 2009). In the finite element methods, they are discretized into 'elements' with irregular geometries and sizes based on the shape and boundary of the tissue (Nielsen et al., 1991; Rogers & McCulloch, 1994; Sack et al., 2018; Vigmond et al., 2002). In these approaches, the discretized tissue does not resemble how the cells are arranged in actual tissue (Fig. 1*A*), and to facilitate large-scale simulations,

Figure 6. Schematic diagrams illustrating conduction in cardiac tissue
A, action potential conduction in normal tissue. *B*, action potential conduction in diseased tissue. Dashed arrows indicated weakened or failed conduction.

the computational cells or elements are usually much larger than the actual myocytes. While the advantage of the continuous models is to allow large-scale computer simulations and facilitate theory development, ignoring the ultrastructural details may impact the prediction power of the models or even give rise to incorrect predictions, particularly in disease conditions where ultrastructural remodelling may become non-trivial for cardiac conduction and arrhythmogenesis.

On the other hand, discretized tissue models consisting of myocytes with realistic geometries and sizes have been developed (Hubbard & Henriquez, 2012; Hubbard et al., 2007; Spach & Heidlage, 1995; Spach et al., 2000). While one can implement the microscopic/ultrastructural details into this type of model [for example, Jæger et al. (2023) used very high spatial (0.5 nm) and temporal (0.02 ns) resolutions with ultrastructural details to simulate a two-cell system], this also causes problems and challenges in modelling and simulations for large-tissue or whole-organ simulations that are needed for investigating cardiac conduction and arrhythmogenesis. In other words, it is computationally challenging to scale up the conduction behaviours at the microscopic (subcellular and small tissue size) to macroscopic (large tissue and whole-heart) levels. Here we briefly discuss the problems and challenges, and what needs to be done in the future.

As shown in many simulation studies, heterogeneous subcellular localizations of Cx43 and $Na_v1.5$ play important roles in conduction in both gap junction and ephaptic coupling. Although T-tubules have been phenomenologically modelled in many computer models, few modelling studies have been carried out to investigate how T-tubular structure affects intracellular action potential depolarization and conduction (Vermij et al., 2019). It is well known that altered T-tubular network structure affects intracellular Ca^{2+} release, yet how it affects action potential conduction is less known. Experimental evidence showed that the T-tubular network may play an important role in action potential conduction (Fig. 3*C*). In real cardiac tissue, myocytes are not arranged as bricks in a brick wall, but in a much more complex and irregular manner (Fig. 1*A*). As shown in computer simulations, heterogeneous Cx43 localization alone combined with irregular arrangements of myocytes can result in complex intracellular conduction patterns (Fig. 4). Therefore, one can imagine the following conduction scenarios by considering the subcellular heterogeneities of Cx43, Na^+ channel and T-tubular network (Fig. 6):
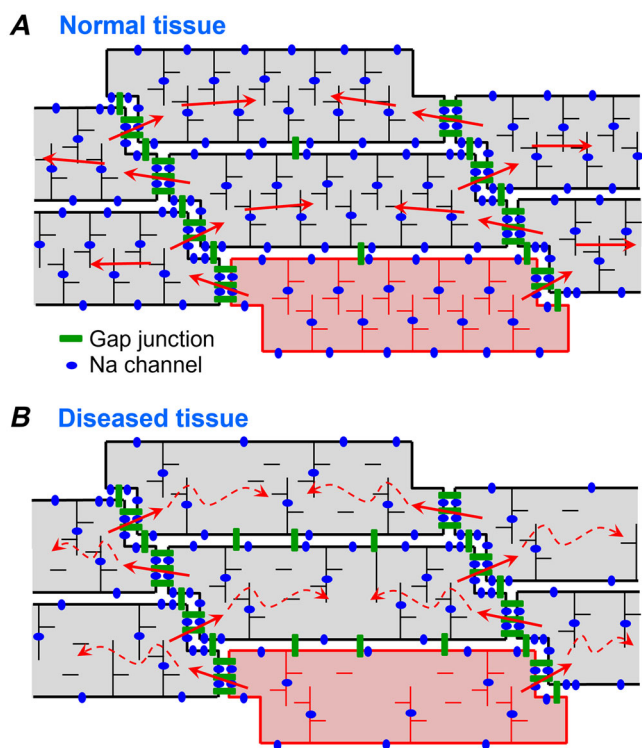
(1) Under normal conditions (Fig. 6*A*), Cx43 is mainly distributed at the cell ends and $Na_v1.5$ density is higher at the cell ends. When one myocyte (the red one) depolarizes, it causes depolarization of the two adjacent cells (following the red arrows)

through the end-to-end connection with either gap junction coupling or ephaptic coupling. These two cells then cause depolarization of the cell above the red cell, resulting in action potential conduction toward the cell centre from the two ends. This process continues, resulting in regenerative conduction in tissue. Although the cells are only coupled end-to-end (longitudinally), due to the manner of cell connection, an effective transverse conduction is realized. In this case, the anisotropic ratio is mainly determined by the geometry of the cell arrangement.

(2) Under diseased conditions (Fig. 6*B*), such as heart failure, T-tubule density is reduced and Cx43 localization is remodelled. As a consequence, the action potential may not be able to conduct throughout the cell (dashed arrows) but can still

conduct from cell to cell (the solid red arrows). Failure of intracellular action potential conduction may attenuate Ca^{2+} release and thus contraction, but electrical conduction can still succeed in the tissue.

Under both scenarios, conduction is impacted by the volume of the cleft or perinexus. In the absence of gap junction coupling (i.e. ephaptic coupling only), conduction fails when this volume is either too small or too large. In the presence of gap junction coupling, conduction is affected by the cleft volume when it is small. This is because activation of the Na^+ channel lowers the Na^+ concentration in the cleft space, which lowers the driving force of I_{Na} to weaken conduction. When the cleft volume is sufficiently large, the change of Na^+ concentration becomes negligible and thus does
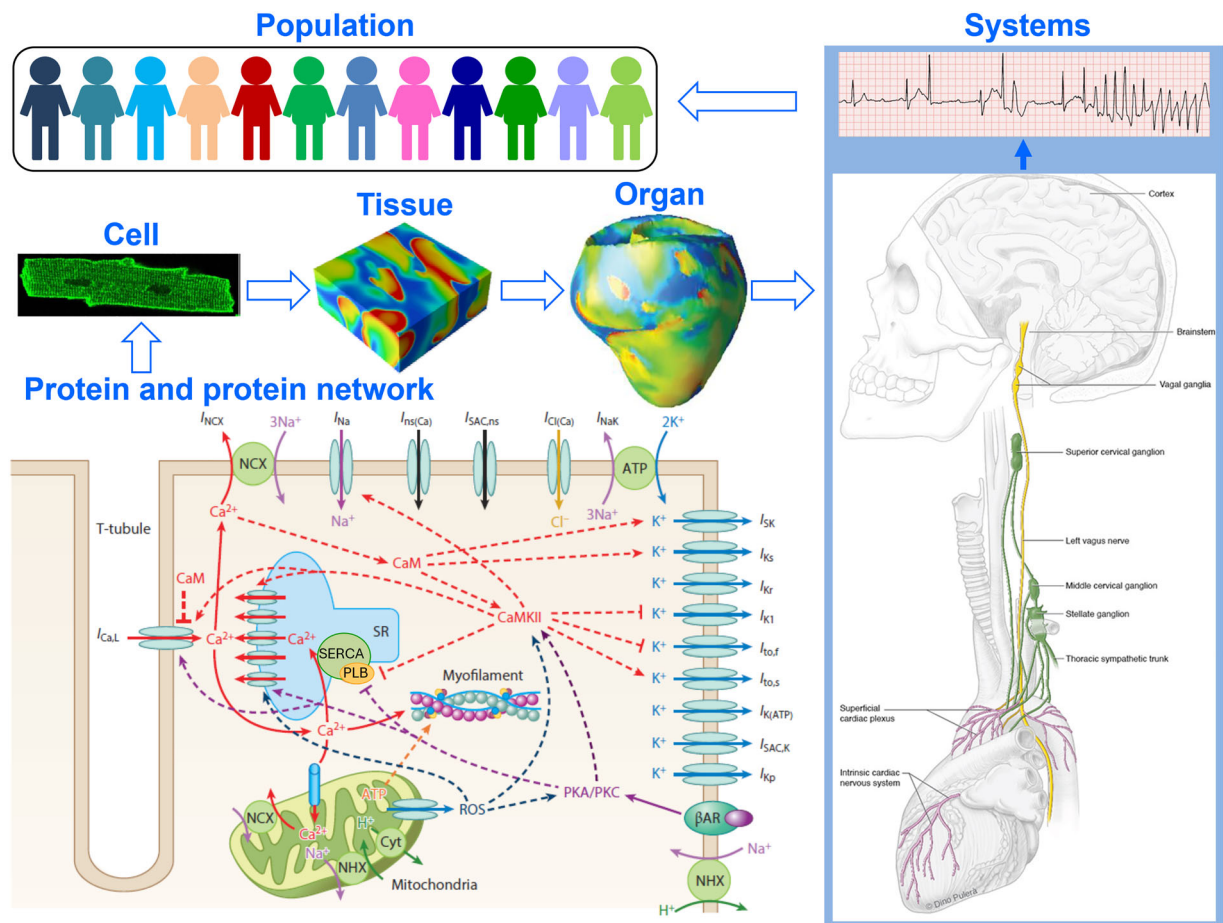
Figure 7. Schematic diagram illustrating multi-scale regulation of cardiac conduction and excitation–contraction coupling
At the molecular and subcellular scale, a genetic mutation or a drug may alter the protein/signalling network and the localization of the proteins. At the cellular scale, the molecular and subcellular changes alter the action potential dynamics and Ca^{2+} cycling. At the tissue and organ scale, the coupling of cells gives rise to tissue-scale phenomena (such as conduction and re-entry), which are affected by the ultrastructural details occurring at the molecular, subcellular and cellular scales. At the systems scales, interactions between different organs (such as the brain and kidney) via the nervous system or chemicals give rise to the systems-level phenomena (such as ECG or symptoms of diseases). At the population scale, a genetic mutation or a drug may exhibit an effect on one individual but not another.

not affect the gap junction-mediated conduction. Besides Na^+, change in K^+ in the cleft may affect the driving force of K^+ currents which may also impact depolarization and repolarization. Besides the volume of the cleft space, whether the extracellular volume of the T-tubules has a role in depolarization or repolarization is unknown. Experiments have shown that the luminal diameter of T-tubules ranges from 20 to 450 nm (Hong & Shaw, 2017). In general, it is not clear whether the ion concentrations in the extracellular space change during the action potential, particularly in fibrotic tissue, where the extracellular volume is reduced. Another largely ignored structural detail in cardiac tissue modelling is neuro-myocyte interactions. Although the neural effects are modelled via β-adrenergic, cholinergic and other signalling pathways, no computer modelling studies have been carried out to simulate the structural details of neuro-myocyte interactions, such as neuromuscular junctions (Franzoso et al., 2022; Zaglia & Mongillo, 2017).

Cardiac conduction and arrhythmias are tissue-scale phenomena, which cannot be fully understood using single cells or small tissue models of a few coupled cells. A reasonable tissue size and geometry are needed to reveal the tissue-scale phenomena, such as re-entry. It is computationally feasible to include the subcellular heterogeneities in a single cell or a small tissue model of coupled cells, but this may be computationally challenging, if not impossible, for large-tissue or whole-organ simulations. However, genetic changes or therapeutic targets are at the molecular scales, yet the molecular effects or readouts on medical consequences are at the organ and systems scales (such as ECG) or at the population scale (such as epidemiology of diseases) (Fig. 7). While continuous models are computationally more tractable, a molecular-level change may result in changes in heterogeneities at the microscopic (cellular and subcellular) scales that cannot be ignored as in continuous models via coarse graining or smoothing. Multiscale modelling approaches need to be developed and employed for such complex medical problems (Qu et al., 2011, 2022). More importantly, different scales of experimental observations are needed to provide data and validations for multiscale modelling.

Synopsis

Cardiac conduction, E–C coupling and arrhythmias are tissue- and organ-scale phenomena that may not be correctly or accurately described by the continuous models that have been used widely by the modelling community thus far. The continuous models have ignored the microscopic (subcellular and cellular) structural details via coarse graining or smoothing, and thus discretized models taking into account the microscopic details from recent experimental advances are now needed. However, this is not computationally tractable at the organ and systems levels and therefore novel computational approaches need to be developed. More importantly, different scales of experimental data and observations are needed to provide data and validations for multiscale modelling.

References

Adams, W. P., Raisch, T. B., Zhao, Y., Davalos, R., Barrett, S., King, D. R., Bain, C. B., Colucci-Chang, K., Blair, G. A., Hanlon, A., Lozano, A., Veeraraghavan, R., Wan, X., Deschenes, I., Smyth, J. W., Hoeker, G. S., Gourdie, R. G., & Poelzing, S (2023). Extracellular perinexal separation is a principal determinant of cardiac conduction. *Circulation Research*, **133**(8), 658–673.

Ajijola, O. A., Yagishita, D., Patel, K. J., Vaseghi, M., Zhou, W., Yamakawa, K., So, E., Lux, R. L., Mahajan, A., & Shivkumar, K. (2013). Focal myocardial infarction induces global remodeling of cardiac sympathetic innervation: Neural remodeling in a spatial context. *American Journal of Physiology-Heart and Circulatory Physiology*, **305**(7), H1031–H1040.

Arora, R., Aistrup, G. L., Supple, S., Frank, C., Singh, J., Tai, S., Zhao, A., Chicos, L., Marszalec, W., Guo, A., Song, L.-S., & Wasserstrom, J. A. (2017). Regional distribution of T-tubule density in left and right atria in dogs. *Heart Rhythm*, **14**(2), 273–281.

Atkinson, A., Inada, S., Li, J., Tellez, J. O., Yanni, J., Sleiman, R., Allah, E. A., Anderson, R. H., Zhang, H., Boyett, M. R., & Dobrzynski, H. (2011). Anatomical and molecular mapping of the left and right ventricular His–Purkinje conduction networks. *Journal of Molecular and Cellular Cardiology*, **51**(5), 689–701.

Blair, G. A., Wu, X., Bain, C., Warren, M., Hoeker, G. S., & Poelzing, S. (2024). Mannitol and hyponatremia regulate cardiac ventricular conduction in the context of sodium channel loss of function. *American Journal of Physiology-Heart and Circulatory Physiology*, **326**(3), H724–H734.

Boyden, P. A., Albala, A., & Dresdner, K. P. (1989). Electro-physiology and ultrastructure of canine subendocardial Purkinje cells isolated from control and 24-hour infarcted hearts. *Circulation Research*, **65**(4), 955–970.

Brandenburg, S., Kohl, T., Williams, G. S. B., Gusev, K., Wagner, E., Rog-Zielinska, E. A., Hebisch, E., Dura, M., Didié, M., Gotthardt, M., Nikolaev, V. O., Hasenfuss, G., Kohl, P., Ward, C. W., Lederer, W. J., & Lehnart, S. E. (2016). Axial tubule junctions control rapid calcium signaling in atria. *Journal of Clinical Investigation*, **126**(10), 3999–4015.

Brette, F., & Orchard, C. (2003). T-tubule function in mammalian cardiac myocytes. *Circulation Research*, **92**(11), 1182–1192.

Brette, F., & Orchard, C. (2007). Resurgence of cardiac t-tubule research. *Physiology (Bethesda, Md.)*, **22**, 167–173.

Brette, F., & Orchard, C. H. (2006). Density and sub-cellular distribution of cardiac and neuronal sodium channel isoforms in rat ventricular myocytes. *Biochemical and Biophysical Research Communications*, **348**(3), 1163–1166.

Camelliti, P., Borg, T. K., & Kohl, P. (2005). Structural and functional characterisation of cardiac fibroblasts. *Cardiovascular Research*, **65**(1), 40–51.

Cao, J. M., Chen, L. S., KenKnight, B. H., Ohara, T., Lee, M. H., Tsai, J., Lai, W. W., Karagueuzian, H. S., Wolf, P. L., Fishbein, M. C., & Chen, P. S. (2000). Nerve sprouting and sudden cardiac death. *Circulation Research*, **86**(7), 816–821.

Chang, C. M., Wu, T. J., Zhou, S., Doshi, R. N., Lee, M. H., Ohara, T., Fishbein, M. C., Karagueuzian, H. S., Chen, P. S., & Chen, L. S. (2001). Nerve sprouting and sympathetic hyperinnervation in a canine model of atrial fibrillation produced by prolonged right atrial pacing. *Circulation*, **103**(1), 22–25.

Chen, F., Mottino, G., Klitzner, T. S., Philipson, K. D., & Frank, J. S. (1995). Distribution of the Na^+/Ca^{2+} exchange protein in developing rabbit myocytes. *American Journal of Physiology-Cell Physiology*, **268**(5), C1126–C1132.

Dajani, A.-H. J., Liu, M. B., Olaopa, M. A., Cao, L., Valenzuela-Ripoll, C., Davis, T. J., Poston, M. D., Smith, E. H., Contreras, J., Pennino, M., Waldmann, C. M., Hoover, D. B., Lee, J. T., Jay, P. Y., Javaheri, A., Slavik, R., Qu, Z., & Ajijola, O. A. (2023). Heterogeneous cardiac sympathetic innervation gradients promote arrhythmogenesis in murine dilated cardiomyopathy. *Journal of Clinical Investigation Insight*, **8**(22), e157956.

Delmar, M., & Liang, F.-X. (2012). Connexin43 and the regulation of intercalated disc function. *Heart Rhythm*, **9**(5), 835–838.

Desplantez, T., Dupont, E., Severs, N. J., & Weingart, R. (2007). Gap junction channels and cardiac impulse propagation. *Journal of Membrane Biology*, **218**(1–3), 13–28.

di Maio, A., Ter Keurs, H. E., & Franzini-Armstrong, C. (2007). T-tubule profiles in Purkinje fibres of mammalian myocardium. *Journal of Muscle Research and Cell Motility*, **28**, 115–121.

Franzoso, M., Dokshokova, L., Vitiello, L., Zaglia, T., & Mongillo, M. (2022). Tuning the consonance of microscopic neuro-cardiac interactions allows the heart beats to play countless genres. *Frontiers in Physiology*, **13**, 841740.

Frisk, M., Koivumäki, J. T., Norseng, P. A., Maleckar, M. M., Sejersted, O. M., & Louch, W. E. (2014). Variable T-tubule organization and Ca^{2+} homeostasis across the atria. *American Journal of Physiology-Heart and Circulatory Physiology*, **307**(4), H609–H620.

Fukuda, K., Kanazawa, H., Aizawa, Y., Ardell, J. L., & Shivkumar, K. (2015). Cardiac innervation and sudden cardiac death. *Circulation Research*, **116**(12), 2005–2019.

George, S. A., Bonakdar, M., Zeitz, M., Davalos, R. V., Smyth, J. W., & Poelzing, S. (2016). Extracellular sodium dependence of the conduction velocity-calcium relationship: Evidence of ephaptic self-attenuation. *American Journal of Physiology-Heart and Circulatory Physiology*, **310**(9), H1129–H1139.

Glukhov, A. V., Balycheva, M., Sanchez-Alonso, J. L., Ilkan, Z., Alvarez-Laviada, A., Bhogal, N., Diakonov, I., Schobesberger, S., Sikkel, M. B., Bhargava, A., Faggian, G., Punjabi, P. P., Houser, S. R., & Gorelik, J. (2015). Direct evidence for microdomain-specific localization and remodeling of functional L-type calcium channels in rat and human atrial myocytes. *Circulation*, **132**(25), 2372–2384.

Gourdie, R. G. (2019). The cardiac gap junction has discrete functions in electrotonic and ephaptic coupling. *The Anatomical Record*, **302**(1), 93–100.

Greer-Short, A., George, S. A., Poelzing, S., & Weinberg, S. H. (2017). Revealing the concealed nature of long-QT type 3 syndrome. *Circulation: Arrhythmia and Electrophysiology*, **10**(2), e004400.

Guo, A., Zhang, C., Wei, S., Chen, B., & Song, L.-S. (2013). Emerging mechanisms of T-tubule remodelling in heart failure. *Cardiovascular Research*, **98**(2), 204–215.

Hesketh, G. G., Shah, M. H., Halperin, V. L., Cooke, C. A., Akar, F. G., Yen, T. E., Kass, D. A., Machamer, C. E., Van Eyk, J. E., & Tomaselli, G. F. (2010). Ultrastructure and Regulation of Lateralized Connexin43 in the Failing Heart. *Circulation Research* **106**(6), 1153–1163.

Hichri, E., Abriel, H., & Kucera, J. P. (2018). Distribution of cardiac sodium channels in clusters potentiates ephaptic interactions in the intercalated disc. *The Journal of Physiology*, **596**(4), 563–589.

Hodgkin, A. L., & Huxley, A. F. (1952). A quantitative description of membrane current and its application to conduction and excitation in nerve. *The Journal of Physiology*, **117**(4), 500–544.

Hong, T., & Shaw, R. M. (2017). Cardiac T-tubule micro-anatomy and function. *Physiological Reviews*, **97**(1), 227–252.

Hooks, D. A., Tomlinson, K. A., Marsden, S. G., LeGrice, I. J., Smaill, B. H., Pullan, A. J., & Hunter, P. J. (2002). Cardiac microstructure: Implications for electrical propagation and defibrillation in the heart. *Circulation Research*, **91**(4), 331–338.

Hooks, D. A., Trew, M. L., Caldwell, B. J., Sands, G. B., LeGrice, I. J., & Smaill, B. H. (2007). Laminar arrangement of ventricular myocytes influences electrical behavior of the heart. *Circulation Research*, **101**(10), e103–112.

Hoyt, R. H., Cohen, M. L., & Saffitz, J. E. (1989). Distribution and three-dimensional structure of intercellular junctions in canine myocardium. *Circulation Research*, **64**(3), 563–574.

Hubbard, M. L., & Henriquez, C. S. (2012). Microscopic variations in interstitial and intracellular structure modulate the distribution of conduction delays and block in cardiac tissue with source-load mismatch. *Europace*, **14**, (Suppl 5), v3–v9.

Hubbard, M. L., Ying, W., & Henriquez, C. S. (2007). Effect of gap junction distribution on impulse propagation in a monolayer of myocytes: A model study. *Europace*, **9**, (Suppl 6), vi20–vi28.

Ivanovic, E., & Kucera, J. P. (2021). Localization of Na+ channel clusters in narrowed perinexi of gap junctions enhances cardiac impulse transmission via ephaptic coupling: A model study. *The Journal of Physiology*, **599**(21), 4779–4811.

Ivanovic, E., & Kucera, J. P. (2022). Tortuous cardiac inter-calated discs modulate ephaptic coupling. *Cells*, **11**(21), 3477.

Jæger, K. H., Ivanovic, E., Kucera, J. P., & Tveito, A. (2023). Nano-scale solution of the Poisson-Nernst-Planck (PNP) equations in a fraction of two neighboring cells reveals the magnitude of intercellular electrochemical waves. *PLoS Computational Biology*, **19**(2), e1010895.

Jansen, J. A., Noorman, M., Musa, H., Stein, M., de Jong, S., van der Nagel, R., Hund, T. J., Mohler, P. J., Vos, M. A., van Veen, T. A., de Bakker, J. M., Delmar, M., & van Rijen, H. V. (2012). Reduced heterogeneous expression of Cx43 results in decreased Nav1.5 expression and reduced sodium current that accounts for arrhythmia vulnerability in conditional Cx43 knockout mice. *Heart Rhythm*, **9**(4), 600–607.

Kaufmann, S. G., Westenbroek, R. E., Maass, A. H., Lange, V., Renner, A., Wischmeyer, E., Bonz, A., Muck, J., Ertl, G., Catterall, W. A., Scheuer, T., & Maier, S. K. G. (2013). Distribution and function of sodium channel subtypes in human atrial myocardium. *Journal of Molecular and Cellular Cardiology*, **61**, 133–141.

Kawano, H., Okada, R., & Yano, K. (2003). Histological study on the distribution of autonomic nerves in the human heart. *Heart and Vessels*, **18**(1), 32–39.

Kirk, M. M., Izu, L T., Chen-Izu, Y., Mcculle, S. L., Wier, W. G., Balke, C. W., & Shorofsky, S. R. (2003). Role of the transverse-axial tubule system in generating calcium sparks and calcium transients in rat atrial myocytes. *The Journal of Physiology*, **547**(2), 441–451.

Kucera, J. P., Rohr, S., & Rudy, Y. (2002). Localization of sodium channels in intercalated disks modulates cardiac conduction. *Circulation Research*, **91**(12), 1176–1182.

Legato, M. J. (1973). Ultrastructure of the atrial, ventricular, and purkinje cell, with special reference to the genesis of arrhythmias. *Circulation*, **47**(1), 178–189.

Leo-Macias, A., Agullo-Pascual, E., & Delmar, M. (2016). The cardiac connexome: Non-canonical functions of connexin43 and their role in cardiac arrhythmias. *Seminars in Cell & Developmental Biology*, **50**, 13–21.

Leo-Macias, A., Agullo-Pascual, E., Sanchez-Alonso, J L., Keegan, S., Lin, X., Arcos, T., Feng-Xia-Liang, Korchev, Y E., Gorelik, J., Fenyö, D., Rothenberg, E., & Delmar, M. (2016). Nanoscale visualization of functional adhesion/excitability nodes at the intercalated disc. *Nature Communications*, **7**(1), 10342.

Leo-Macías, A., Liang, F.-X., & Delmar, M. (2015). Ultrastructure of the intercellular space in adult murine ventricle revealed by quantitative tomographic electron microscopy. *Cardiovascular Research*, **107**, 442–452.

Lieu, D. K., Liu, J., Siu, C.-W., McNerney, G. P., Tse, H.-F., Abu-Khalil, A., Huser, T., & Li, R. A. (2009). Absence of transverse tubules contributes to non-uniform Ca^{2+} wave-fronts in mouse and human embryonic stem cell–derived cardiomyocytes. *Stem Cells and Development*, **18**(10), 1493–1500.

Lin, J., & Keener, J. P. (2010). Modeling electrical activity of myocardial cells incorporating the effects of ephaptic coupling. *Proceedings National Academy of Science USA*, **107**(49), 20935–20940.

Lin, X., Liu, N., Lu, J., Zhang, J., Anumonwo, J. M. B., Isom, L. L., Fishman, G. I., & Delmar, M. (2011). Subcellular heterogeneity of sodium current properties in adult cardiac ventricular myocytes. *Heart Rhythm*, **8**(12), 1923–1930.

Lipp, P., Hüser, J., Pott, L., & Niggli, E. (1996). Spatially non-uniform Ca^{2+} signals induced by the reduction of transverse tubules in citrate-loaded guinea-pig ventricular myocytes in culture. *The Journal of Physiology*, **497**(3), 589–597.

Liu, B. R., & Cherry, E. M. (2015). Image-based structural modeling of the cardiac Purkinje network. *BioMed Research International*, **2015**, 1.

Liu, J., Lieu, D. K., Siu, C. W., Fu, J.-D., Tse, H.-F., & Li, R. A. (2009). Facilitated maturation of Ca^{2+} handling properties of human embryonic stem cell-derived cardio-myocytes by calsequestrin expression. *American Journal of Physiology-Cell Physiology*, **297**(1), C152–C159.

Liu, M. B., Vandersickel, N., Panfilov, A. V., & Qu, Z. (2019). R-from-T as a common mechanism of arrhythmia initiation in long QT syndromes. *Circulation: Arrhythmia and Electro-physiology*, **12**(12), e007571.

Ly, C., & Weinberg, S. H. (2022). Automaticity in ventricular myocyte cell pairs with ephaptic and gap junction coupling. *Chaos: An Interdisciplinary Journal of Nonlinear Science*, **32**(3), 033123.

Lyon, A. R., MacLeod, K. T., Zhang, Y., Garcia, E., Kanda, G. K., Lab, M. J., Korchev, Y. E., Harding, S. E., & Gorelik, J. (2009). Loss of T-tubules and other changes to surface topography in ventricular myocytes from failing human and rat heart. *Proceedings National Academy of Science USA*, **106**(16), 6854–6859.

Maier, S. K. G., Westenbroek, R. E., McCormick, K. A., Curtis, R., Scheuer, T., & Catterall, W. A. (2004). Distinct sub-cellular localization of different sodium channel α and β subunits in single ventricular myocytes from mouse heart. *Circulation*, **109**(11), 1421–1427.

Maier, S. K. G., Westenbroek, R. E., Schenkman, K. A., Feigl, E. O., Scheuer, T., & Catterall, W. A. (2002). An unexpected role for brain-type sodium channels in coupling of cell surface depolarization to contraction in the heart. *Proceedings National Academy of Science USA*, **99**(6), 4073–4078.

Martins-Marques, T., Catarino, S., Gonçalves, A., Miranda-Silva, D., Gonçalves, L., Antunes, P., Coutinho, G., Leite Moreira, A., Falcão Pires, I., & Girão, H. (2020). EHD1 modulates Cx43 gap junction remodeling associated with cardiac diseases. *Circulation Research*, **126**(10), e97–e113.

Moise, N., Struckman, H. L., Dagher, C., Veeraraghavan, R., & Weinberg, S. H. (2021). Intercalated disk nanoscale structure regulates cardiac conduction. *Journal of General Physiology*, **153**(8), e202112897.

Mori, Y., Fishman, G. I., & Peskin, C. S. (2008). Ephaptic conduction in a cardiac strand model with 3D electro-diffusion. *Proceedings National Academy of Science USA*, **105**(17), 6463–6468.

Nielsen, M. S., van Opbergen, C. J. M., van Veen, T.A.B., & Delmar, M. (2023). The intercalated disc: A unique organelle for electromechanical synchrony in cardio-myocytes. *Physiological Reviews*, **103**(3), 2271–2319.

Nielsen, P. M. F., Grice, I. J. L., Smaill, B. H., & Hunter, P. J. (1991). Mathematical model of geometry and fibrous structure of the heart. *American Journal of Physiology*, **260**, H1365–H1378.

Nivala, M., Song, Z., Weiss, J. N., & Qu, Z. (2015). T-tubule disruption promotes calcium alternans in failing ventricular myocytes: Mechanistic insights from computational modeling. *Journal of Molecular and Cellular Cardiology*, **79**, 32–41.

Nowak, M. B., Greer-Short, A., Wan, X., Wu, X., Deschênes, I., Weinberg, S. H., & Poelzing, S. (2020). Intercellular sodium regulates repolarization in cardiac tissue with sodium channel gain of function. *Biophysical Journal*, **118**(11), 2829–2843.

Nowak, M. B., Poelzing, S., & Weinberg, S. H. (2021). Mechanisms underlying age-associated manifestation of cardiac sodium channel gain-of-function. *Journal of Molecular and Cellular Cardiology*, **153**, 60–71.

Peters, N. S., & Wit, A. L. (1998). Myocardial architecture and ventricular arrhythmogenesis. *Circulation*, **97**(17), 1746–1754.

Petitprez, S., Zmoos, A.-F., Ogrodnik, J., Balse, E., Raad, N., El-Haou, S., Albesa, M., Bittihn, P., Luther, S., Lehnart, S. E., Hatem, S. N., Coulombe, A., & Abriel, H. (2011). SAP97 and dystrophin macromolecular complexes determine two pools of cardiac sodium channels Na$_v$1.5 in cardiomyocytes. *Circulation Research*, **108**(3), 294–304.

Pinali, C., Bennett, H. J., Davenport, J. B., Caldwell, J. L., Starborg, T., Trafford, A. W., & Kitmitto, A. (2015). Three-dimensional structure of the intercalated disc reveals plicate domain and gap junction remodeling in heart failure. *Biophysical Journal*, **108**(3), 498–507.

Qu, Z., Garfinkel, A., Weiss, J. N., & Nivala, M. (2011). Multi-scale modeling in biology: How to bridge the gaps between scales? *Progress in Biophysics and Molecular Biology*, **107**(1), 21–31.

Qu, Z., Hu, G., Garfinkel, A., & Weiss, J. N. (2014). Non-linear and stochastic dynamics in the heart. *Physics Reports*, **543**(2), 61–162.

Qu, Z., Yan, D., & Song, Z (2022). Modeling calcium cycling in the heart: Progress, pitfalls, and challenges. *Biomolecules*, **12**(11), 1686.

Raisch, T. B., Yanoff, M. S., Larsen, T. R., Farooqui, M. A., King, D. R., Veeraraghavan, R., Gourdie, R. G., Baker, J. W., Arnold, W. S., AlMahameed, S. T., & Poelzing, S. (2018). Intercalated disk extracellular nanodomain expansion in patients with atrial fibrillation. *Frontiers in Physiology*, **9**, 398.

Rhett, J. M., & Gourdie, R. G. (2012). The perinexus: A new feature of Cx43 gap junction organization. *Heart Rhythm*, **9**(4), 619–623.

Rhett, J. M., Jourdan, J., & Gourdie, R. G. (2011). Connexin 43 connexon to gap junction transition is regulated by zonula occludens-1. *Molecular Biology of the Cell*, **22**(9), 1516–1528.

Rhett, J. M., Ongstad, E. L., Jourdan, J., & Gourdie, R. G. (2012). Cx43 associates with Nav1.5 in the cardiomyocyte perinexus. *Journal of Membrane Biology*, **245**(7), 411–422.

Rhett, J. M., Veeraraghavan, R., Poelzing, S., & Gourdie, R. G. (2013). The perinexus: Sign-post on the path to a new model of cardiac conduction? *Trends in Cardiovascular Medicine*, **23**(6), 222–228.

Richards, M. A., Clarke, J. D., Saravanan, P., Voigt, N., Dobrev, D., Eisner, D. A., Trafford, A. W., & Dibb, K. M. (2011). Transverse tubules are a common feature in large mammalian atrial myocytes including human. *American Journal of Physiology-Heart and Circulatory Physiology*, **301**(5), H1996–H2005.

Rivaud, M. R., Agullo-Pascual, E., Lin, X., Leo-Macias, A., Zhang, M., Rothenberg, E., Bezzina, C. R., Delmar, M., & Remme, C. A. (2017). Sodium channel remodeling in subcellular microdomains of murine failing cardiomyocytes. *Journal of the American Heart Association*, **6**(12), e007622.

Rogers, J. M., & McCulloch, A. D. (1994). A collocation-Galerkin finite element model of cardiac action potential propagation. *IEEE Transactions on Biomedical Engineering*, **41**(8), 743–757.

Sacconi, L., Ferrantini, C., Lotti, J., Coppini, R., Yan, P., Loew, L. M., Tesi, C., Cerbai, E., Poggesi, C., & Pavone, F. S. (2012). Action potential propagation in transverse-axial tubular system is impaired in heart failure. *Proceedings of the National Academy of Sciences of the USA*, **109**(15), 5815–5819.

Sachse, F. B., Torres, N. S., Savio-Galimberti, E., Aiba, T, Kass, D. A., Tomaselli, G. F., & Bridge, J. H. (2012). Subcellular structures and function of myocytes impaired during heart failure are restored by cardiac resynchronization therapy. *Circulation Research*, **110**(4), 588–597.

Sack, K. L., Aliotta, E., Ennis, D. B., Choy, J. S., Kassab, G. S., Guccione, J. M., & Franz, T. (2018). Construction and validation of subject-specific biventricular finite-element models of healthy and failing swine hearts from high-resolution DT-MRI. *Frontiers in Physiology*, **9**, 539.

Saffitz, J. E., Hames, K. Y., & Kanno, S. (2007). Remodeling of gap junctions in ischemic and nonischemic forms of heart disease. *Journal of Membrane Biology*, **218**(1–3), 65–71.

Scollan, D. F., Holmes, A., Zhang, J., & Winslow, R. L. (2000). Reconstruction of cardiac ventricular geometry and fiber orientation using magnetic resonance imaging. *Annals of Biomedical Engineering*, **28**(8), 934–944.

Severs, N. J., Bruce, A. F., Dupont, E., & Rothery, S. (2008). Remodelling of gap junctions and connexin expression in diseased myocardium. *Cardiovascular Research*, **80**(1), 9–19.

Severs, N. J., Dupont, E., Coppen, S. R., Halliday, D., Inett, E., Baylis, D., & Rothery, S. (2004). Remodelling of gap junctions and connexin expression in heart disease. *Biochimica et Biophysica Acta (BBA)-Biomembranes*, **1662**(1–2), 138–148.

Soeller, C., & Cannell, M. B. (1999). Examination of the transverse tubular system in living cardiac rat myocytes by 2-photon microscopy and digital image–processing techniques. *Circulation Research*, **84**(3), 266–275.

Song, L. S., Sobie, E. A., McCulle, S., Lederer, W. J., Balke, C. W., & Cheng, H. (2006). Orphaned ryanodine receptors in the failing heart. *Proceedings National Academy of Science USA*, **103**(11), 4305–4310.

Song, Z., Liu, M. B., & Qu, Z. (2018). Transverse tubular network structures in the genesis of intracellular calcium alternans and triggered activity in cardiac cells. *Journal of Molecular and Cellular Cardiology*, **114**, 288–299.

Spach, M. S., & Heidlage, J. F. (1995). The stochastic nature of cardiac propagation at a microscopic level – electrical description of myocardial architecture and its application to conduction. *Circulation Research*, **76**(3), 366–380.

Spach, M. S., Heidlage, J. F., Dolber, P. C., & Barr, R. C. (2000). Electrophysiological effects of remodeling cardiac gap junctions and cell size – Experimental and model studies of normal cardiac growth. *Circulation Research*, **86**(3), 302–311.

Sperelakis, N (2002). An electric field mechanism for transmission of excitation between myocardial cells. *Circulation Research*, **91**(11), 985–987.

Sperelakis, N., & Mann, J. E. (1977). Evaluation of electric field changes in the cleft between excitable cells. *Journal of Theoretical Biology*, **64**(1), 71–96.

Streeter, D. D., Spotnitz, H. M., Patel, D. P., Ross, J., & Sonnenblick, E. H. (1969). Fiber orientation in the canine left ventricle during diastole and systole. *Circulation Research* **24**(3), 339–347.

Thaemert, J. C. (1970). Atrioventricular node innervation in ultrastructural three dimensions. *American Journal of Anatomy*, **128**(2), 239–263.

Trayanova, N. A. (2011). Whole-heart modeling: Applications to cardiac electrophysiology and electromechanics. *Circulation Research*, **108**(1), 113–128.

Vanslembrouck, B., Kremer, A., Van Roy, F., Lippens, S., & van Hengel, J. (2020). Unravelling the ultrastructural details of αT-catenin-deficient cell–cell contacts between heart muscle cells by the use of FIB-SEM. *Journal of Microscopy*, **279**(3), 189–196.

Veeraraghavan, R., Lin, J., Hoeker, G. S., Keener, J. P., Gourdie, R. G., & Poelzing, S. (2015). Sodium channels in the Cx43 gap junction perinexus may constitute a cardiac ephapse: An experimental and modeling study. *Pflügers Archiv-European Journal of Physiology*, **467**(10), 2093–2105.

Veeraraghavan, R., Lin, J., Keener, J. P., Gourdie, R., & Poelzing, S. (2016). Potassium channels in the Cx43 gap junction perinexus modulate ephaptic coupling: An experimental and modeling study. *Pflügers Archiv-European Journal of Physiology*, **468**(10), 1651–1661.

Vermij, S. H., Abriel, H., & Kucera, J. P. (2019). Modeling depolarization delay, sodium currents, and electrical potentials in cardiac transverse tubules. *Frontiers in Physiology*, **10**, 1487.

Vigmond, E. J., Aguel, F., & Trayanova, N. A. (2002). Computational techniques for solving the bidomain equations in three dimensions. *IEEE Transactions on Bio-Medical Engineering*, **49**(11), 1260–1269.

Vreeker, A., van Stuijvenberg, L., Hund, T. J., Mohler, P. J., Nikkels, P. G. J. & van Veen, T. A. B. (2014). Assembly of the cardiac intercalated disk during pre- and post-natal development of the human heart. *PLoS ONE*, **9**(4), e94722.

Wang, Y., Li, Q., Tao, B., Angelini, M., Ramadoss, S., Sun, B., Wang, P., Krokhaleva, Y., Ma, F., Gu, Y., Espinoza, A., Yamauchi, K., Pellegrini, M., Novitch, B., Olcese, R., Qu, Z., Song, Z., & Deb, A. (2023). Fibroblasts in heart scar tissue directly regulate cardiac excitability and arrhythmogenesis. *Science*, **381**(6665), 1480–1487.

Wei, N., & Tolkacheva, E. G. (2020). Interplay between ephaptic coupling and complex geometry of border zone during acute myocardial ischemia: Effect on arrhythmogeneity. *Chaos: An Interdisciplinary Journal of Nonlinear Science*, **30**(3), 033111.

Weinberg, S. H. (2023). Sodium channel subpopulations with distinct biophysical properties and subcellular localization enhance cardiac conduction. *Journal of General Physiology*, **155**(8), e202313382.

Wu, X., Hoeker, G. S., Blair, G. A., King, D. R., Gourdie, R. G., Weinberg, S. H., & Poelzing, S. (2021). Hypernatremia and intercalated disc edema synergistically exacerbate long-QT syndrome type 3 phenotype. *American Journal of Physiology-Heart and Circulatory Physiology*, **321**(6), H1042–H1055.

Xie, F., Qu, Z., Yang, J., Baher, A., Weiss, J. N., & Garfinkel, A. (2004). A simulation study of the effects of cardiac anatomy in ventricular fibrillation. *Journal of Clinical Investigation*, **113**, 686–693.

Xie, Y., Garfinkel, A., Camelliti, P., Kohl, P., Weiss, J. N., & Qu, Z. (2009). Effects of fibroblast-myocyte coupling on cardiac conduction and vulnerability to reentry: A computational study. *Heart Rhythm*, **6**(11), 1641–1649.

Zaglia, T., & Mongillo, M. (2017). Cardiac sympathetic innervation, from a different point of (re)view. *The Journal of Physiology*, **595**(12), 3919–3930.

Zhang, L., Ina, K., Kitamura, H., Campbell, G. R., & Shimada, T. (1996). The intercalated disc of monkey myocardial cells and purkinje fibers as revealed by scanning electron microscopy. *Archives of Histology and Cytology*, **59**(5), 453–465.

Zhu, C., Rajendran, P. S., Hanna, P., Efimov, I. R., Salama, G., Fowlkes, C. C., & Shivkumar, K. (2022). High-resolution structure-function mapping of intact hearts reveals altered sympathetic control of infarct border zones. *Journal of Clinical Investigation Insight*, **7**(3), e153913.

Additional information

Competing interests

None declared.

Author contributions

Supporting information

Additional supporting information can be found online in the Supporting Information section at the end of the HTML view of the article. Supporting information files available:

Peer Review History